



RESEARCH LETTER

10.1029/2023GL103975

Seasonal Prediction of Arabian Sea Marine Heatwaves

Vimal Koul^{1,2,3} , Sebastian Brune¹ , Anna Akimova⁴, André Düsterhus⁵ , Patrick Pieper⁶,
Laura Hövel⁷, Anant Parekh⁸ , Corinna Schrum^{1,2}, and Johanna Baehr¹

Key Points:

- Summer marine heatwaves in the Arabian Sea are predictable seven months in advance
- The prediction skill in summer is mainly associated with a preceding El Niño event in winter
- Probabilistic predictions of Arabian Sea area under heatwave can be tailored to benefit fisheries

Supporting Information:

Supporting Information may be found in the online version of this article.

Correspondence to:

V. Koul,
vimal.koul@noaa.gov

Citation:

Koul, V., Brune, S., Akimova, A., Düsterhus, A., Pieper, P., Hövel, L., et al. (2023). Seasonal prediction of Arabian Sea marine heatwaves. *Geophysical Research Letters*, 50, e2023GL103975. <https://doi.org/10.1029/2023GL103975>

Received 4 APR 2023
Accepted 30 JUL 2023

Author Contributions:

Conceptualization: Vimal Koul
Data curation: Sebastian Brune, Laura Hövel
Formal analysis: Vimal Koul
Methodology: Vimal Koul, Sebastian Brune, Anna Akimova, André Düsterhus, Patrick Pieper
Supervision: Corinna Schrum, Johanna Baehr
Visualization: Vimal Koul
Writing – original draft: Vimal Koul
Writing – review & editing: Sebastian Brune, Anna Akimova, André Düsterhus, Patrick Pieper, Laura Hövel, Anant Parekh, Corinna Schrum, Johanna Baehr

¹Center for Earth System Sustainability, Institute of Oceanography, Universität Hamburg, Hamburg, Germany, ²Helmholtz Zentrum Hereon, Institute of Coastal Analysis, Geesthacht, Germany, ³Now at Cooperative Institute for Modeling the Earth System, Princeton University, Princeton, NJ, USA, ⁴Thünen Institute of Sea Fisheries, Bremerhaven, Germany, ⁵Department of Geography, Irish Climate Analysis and Research UnitS (ICARUS), Maynooth University, Maynooth, Ireland, ⁶Freie Universität Berlin, Berlin, Germany, ⁷Oeschger Center for Climate Change Research and Institute of Geography, University of Bern, Bern, Switzerland, ⁸Indian Institute of Tropical Meteorology, Ministry of Earth Sciences, Pune, India

Abstract Marine heatwaves are known to have a detrimental impact on marine ecosystems, yet predicting when and where they will occur remains a challenge. Here, using a large ensemble of initialized predictions from an Earth System Model, we demonstrate skill in predictions of summer marine heatwaves over large marine ecosystems in the Arabian Sea seven months ahead. Retrospective forecasts of summer (June to August) marine heatwaves initialized in the preceding winter (November) outperform predictions based on observed frequencies. These predictions benefit from initialization during winters of medium to strong El Niño conditions, which have an impact on marine heatwave characteristics in the Arabian Sea. Our probabilistic predictions target spatial characteristics of marine heatwaves that are specifically useful for fisheries management, as we demonstrate using an example of Indian oil sardine (*Sardinella longiceps*).

Plain Language Summary Marine heatwaves (MHWs) are prolonged extreme events associated with exceptionally high ocean water temperatures. Such events impose heat stress on marine life, and thus predicting such events is beneficial for management applications. In this work we show that the occurrence of MHWs in summer in the Arabian Sea can be skilfully predicted seven month in advance. Our prediction system benefits from the information of sea surface temperature anomalies in the eastern Pacific Ocean in the preceding winter, among other aspects. Our predictions suggest potential for using climate information in fisheries management in this region.

1. Introduction

Marine heatwaves (MHWs) are prolonged extreme events associated with exceptionally high ocean water temperatures (Hobday, Alexander, et al., 2016; Pearce & Feng, 2013). With the increased availability of high resolution ocean observations, MHWs have now been observed in many regional seas and coastal zones. Some prominent events being the Mediterranean Sea MHW of 2003 (Olita et al., 2007), the west Australian MHW of 2011 (Feng et al., 2013), the 2014–2016 MHW in the Northeast Pacific (Bond et al., 2015) and the 2015–2016 MHW in the Tasman Sea (Oliver et al., 2017). The frequency of MHWs over many oceanic regions has increased since the beginning of the observational record and is projected to further increase in the 21st century (Frölicher et al., 2018; Oliver et al., 2019). Recent studies have attributed such long term increase mainly to the anthropogenic warming-driven increase in mean sea surface temperatures (SST) with some contribution from the internal climate variability (Oliver, 2019).

MHWs have well-documented devastating impacts on the well being of living marine resources and ecosystem functions. These impacts include mass coral bleaching (Feng et al., 2013; Hughes et al., 2017), widespread habitat loss through damages to seagrass meadows and kelp forests (Babcock et al., 2019; Filbee-Dexter & Wernberg, 2018), changes in species abundance and distribution, mass stranding and elevated mortality, unprecedented changes in ecosystem community structure (Caputi et al., 2016; Cavole et al., 2016; Smale et al., 2019; Wernberg et al., 2011). MHWs have also been shown to cause shocks in seafood production in various regions of the world ocean which result in dramatic economic losses (Cheung et al., 2021).

The origins and impacts of MHWs have been well studied in many regional seas around the globe, however, a conspicuous gap had remained in our understanding of these extreme events in the Indian Ocean, particularly in its northern coastal regions. Recent studies report a rapid increase in the MHW characteristics in the north Indian

© 2023. The Authors.

This is an open access article under the terms of the [Creative Commons Attribution-NonCommercial-NoDerivs License](https://creativecommons.org/licenses/by/4.0/), which permits use and distribution in any medium, provided the original work is properly cited, the use is non-commercial and no modifications or adaptations are made.

Ocean (Chatterjee et al., 2022; Saranya et al., 2022), with maximum intensity of MHWs exceeding 2°C during the summer season in some years. Like other regions, the MHWs in the Indian Ocean are also mainly associated with the secular increase in the mean SST. Further, various modes of climate variability, such as the El Niño Southern Oscillation (ENSO) and the Indian Ocean Dipole (IOD), also modulate the background climate state from one year to another. Furthermore, superimposed on the background climate state are local surface radiative flux and wind anomalies which play a crucial role in the origin and persistence of the MHWs in the north Indian Ocean (Chatterjee et al., 2022).

While it is understood that timely prediction of MHWs would provide much required early warnings of such events, an assessment of the prediction skill of MHWs in the north Indian Ocean is still missing. In this study, we explore predictability of MHWs and their possible impacts on Arabian Sea large marine ecosystem, which is one of the most productive regions of the world ocean hosting intensive artisanal and commercial fisheries (Andrew et al., 1998). We focus here on the impacts of MHWs on Indian oil sardine (*Sardinella longiceps*), a small pelagic fish that contributes between 15% and 20% of total marine fish catches in India (Kripa et al., 2018; Vivekanandan et al., 2009). Among many other climate stressors, extreme temperatures are known to negatively impact oil sardines (Hamza, Valsala, et al., 2021; Kripa et al., 2018; Sajna et al., 2019). We consider both the occurrence of MHWs and the exceedance of the 28°C temperature threshold together. This threshold is used as an upper limit, beyond which prolonged heat stress can harm oil sardines. A timely prediction of MHWs in the Arabian Sea would allow precautionary measures to be taken to minimise the impact of MHWs on oil sardine fishery.

Here, we assess the prediction skill of MHWs in the Arabian Sea using a global climate prediction system with a focus on the summer season (June-August), which is the main spawning period of the Indian oil sardine. During the spawning season southwesterly monsoon winds initiate coastal upwelling and thus increase productivity along the southeastern and western Arabian Sea. We explore the potential for predictability of MHWs in this region through an analysis of the impact of the El Niño and IOD on prediction skill of MHWs. Our prediction system is initialized in November each year and targets the subsequent summer season (June to August) 7 months later.

2. Methods

2.1. Data and Calculation of Marine Heatwave Characteristics

We use the NOAA OISST version 2 High Resolution Dataset (Banzon et al., 2016) from 1982 to 2019 as observational reference for computing marine heatwave (MHW) characteristics. We apply a widely used and publicly available marine heatwave detection algorithm to the observational data set (Hobday, Alexander, et al., 2016). In this study, we focus on two characteristics: the number of MHW events per summer and the maximum intensity of marine heatwave events per summer. Hence our results concern seasonal (June to August) rather than single event characteristics.

2.2. Area Under Marine Heatwave

Our region of interest is the Arabian Sea which is a regional sea in the Indian Ocean bounded by 50:78°E longitudes and 6:26°N latitudes. Some parts of the Gulf of Aden, the Gulf of Oman, the Persian Gulf and the entire Red Sea are excluded from our definition. To keep the focus on the prediction of living marine resources we consider only those grid cells which conform to the definition of large marine ecosystem (Sherman, 1991). This excludes the deeper southern parts of the Arabian Sea region from the subsequent analysis. The total area of the selected region is about 3,766,700 km². Almost each summer some fraction of this area experiences MHWs. We define a MHW to occur when daily temperatures exceed the 11-day running 90th percentile threshold for at-least five consecutive days (Hobday, Alexander, et al., 2016). The 11-day running 90th percentile is calculated from daily SSTs over the period 1983–2012 and is further smoothed with a 31-day running mean. We calculate the percentage-area where at-least one MHW occurs each summer (event-based area under heatwave), and additionally have intensity larger than temperature threshold of 28°C (event- and intensity-based area under heatwave). The 28°C threshold coincides with the previously reported to be optimal for Indian oil sardine (Benzam, 1970; Vivekanandan et al., 2009). Temperatures above this optimum have been previously suggested to cause physiological stress in fishes and to lead to deficit catches of the sardine fisheries in this region (Hamza, Valsala, et al., 2021).

2.3. The Large-Ensemble Prediction System

We carried out retrospective predictions using the Max Planck Institute Earth System Model in low resolution (Mauritsen et al., 2019, MPI-ESM-LR). The ocean model of MPI-ESM, the MPIOM, has a rotated grid configuration, where the North Pole singularity is moved over Greenland. This improves horizontal resolution in the Atlantic north of 50°N (horizontal resolution in Pacific sector is not improved with the pole over Greenland). We have deployed the same prediction system as described in Koul et al. (2021), however, we now use an extended set of initialized predictions with 80 ensemble members. At the core of the initialization is a 16-member weakly coupled data assimilation combining atmospheric nudging with an oceanic localized ensemble Kalman filter (Brune & Baehr, 2020) using the Parallel Data Assimilation Framework (PDAF, Nerger & Hiller, 2013). To further increase the ensemble size, model physics at upper stratospheric levels are perturbed, similar to the approach described in Fröhlich et al. (2021). Thus, an 80-member ensemble of 10-year long retrospective forecasts (hereafter: hindcasts) is initialized every November 1st from 1982 to 2019. Our target prediction horizon is the first summer (June to August) after initialization which translates to a 7-month lead prediction. Beyond this lead time, there is no skill in our prediction system for the target MHW characteristics. We refer the interested reader to Brune et al. (2015), Brune and Baehr (2020), Hövel et al. (2022), and Koul et al. (2021) for a more detailed explanation on the predictions system and its initialization.

2.4. Reference and Statistical Predictions

We use observed frequency of MHWs as the reference to assess the model prediction skill. The skill (see below) is evaluated against this reference. We also compare our dynamical predictions with predictions from a statistical model. The statistical prediction is the observed frequency of target event conditional on El Niño. We first determine the years when the October-December mean anomalies of the Niño 3.4 index (Table S1 in Supporting Information S1) are above and below +0.5°C. We then calculate the observed frequency of the target event in El Niño (Niño 3.4 > +0.5°C) and Non-El Niño (Niño 3.4 ≤ +0.5°C) years (Table S2 in Supporting Information S1). The statistical prediction for a given summer is then the observed frequency of the target event depending on whether the preceding October-December mean Niño 3.4 anomaly was above or below +0.5°C.

We use the Brier Skill Score (BSS) as the verification metric for our predictions. The BSS is defined as:

$$BSS = 1 - \frac{BS_{prediction}}{BS_{reference}}$$

where, $BS_{prediction}$ is the Brier Score of the 80-member initialized prediction and $BS_{reference}$ is the Brier Score of the reference prediction (i.e., either the observed frequency or the statistical prediction). For calculating the Brier Score, we use the upper tercile of the predictand as the Brier threshold. The uncertainty in the BSS is calculated using a block bootstrap approach (block length = 3) wherein, through random sampling and replacement from the parent time series, a set of 1,000 BSSs is estimated. We select the 90% range of these 1,000 BSSs as a measure of the uncertainty in the estimated BSS. Statistical significance for linear trend and composite differences analyzed in this work are also determined using the bootstrap approach.

3. Results

There is a positive trend in the number of marine heatwaves (MHW) occurring every summer in the Arabian Sea (Figure 1a). In fact, over the last decade (2010–2019), the number of MHW events has more than doubled compared to the first decade (1982–1991) of the observational record (Figure S1 in Supporting Information S1). Large increase has occurred in the eastern Arabian Sea along the entire west coast of India. Within the Arabian Sea, the mean summer SST are warmer in the east than in west (Figure 1b), but this distribution of mean summer SST is distinct from the spatial distribution of MHW characteristics. Eastern and northern regions with relatively warm summer SST are prone to frequent MHW events while the western region characterized by seasonal upwelling is prone to intense MHW events (Figure 1d).

The observed spatial pattern of MHW events and intensity is captured by the prediction system (Figure 2) with the pattern correlation being higher for mean MHW intensity than for MHW events. Overall, as seen in observations, the regions of high MHW events and intensity lie in the eastern and western parts of the Arabian Sea

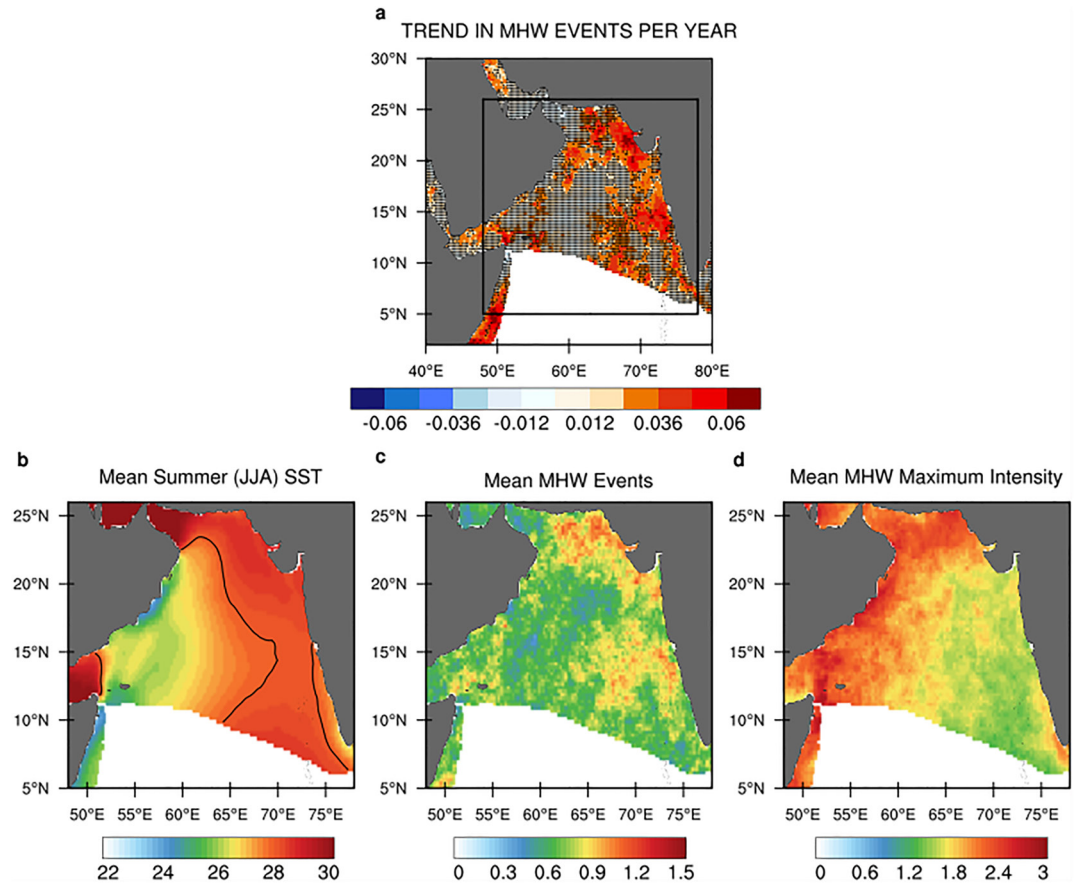


Figure 1. Observed marine heatwave characteristics. (a) Linear trend in summer (June–August) marine heatwave events ($\text{events}/\text{yr}^{-1}$). Trend values that are not significant at 95% confidence are stippled. (b) Climatological mean (1982–2019) summer (June–August mean) sea surface temperature ($^{\circ}\text{C}$), (c) climatological mean MHW events and (d) climatological mean MHW max intensity ($^{\circ}\text{C}$). The black box in (a) shows the region over which the MHW characteristics are averaged. The black line in (b) shows the 28°C contour.

respectively (Figure S2 in Supporting Information S1). From a probabilistic point of view, the prediction system captures the broadly distinct probabilities of MHW characteristics. The tercile-based probability density functions show that the prediction system is able to discriminate summers with extensive MHW activity from the rest (Figures 2c and 2d). This distinction is more clear for the number of MHW events than for their intensity. For example, 62% of all MHW event predictions agree with the observed MHW events in the upper tercile. Also the ensemble shows large spread during summers with extensive MHW activity (Figure S3 in Supporting Information S1), hinting toward an impact of the climate state at initialization.

An analysis of the background climatic state suggests a possible connection of El Niño as well as the IOD with the MHW events in the Arabian Sea (Figure 3). First of all, there is a considerable overlap between the warm phases of the ENSO and positive IOD (IOD+) conditions for the months October to December (Figure 3a and Table S1 in Supporting Information S1). Both of these conditions are known to favor warm SSTs in the Arabian Sea (Chowdary & Gnanaseelan, 2007). A warm ENSO anomaly ($>0.5^{\circ}\text{C}$) in winter makes MHW events more likely over the Arabian Sea (Figure 3b and Table S2 in Supporting Information S1). Positive IOD conditions also favor MHW events in the entire Arabian Sea, however, the impact is small in comparison to the impact of El Niño (Figure 3c). Toward the end of the last decade, a number of positive IOD events in winter were not succeeded by MHW events (Figure 3a). In summary, the likelihood of an MHW event to occur is higher than the climatological frequency in summers which are preceded by El Niño (or IOD+) conditions in winter (Tables S2 and S3 in Supporting Information S1).

In the observational record large areas of the Arabian Sea have been under the influence of MHW in summer even in the absence of an El Niño or an IOD+ event in the preceding winter (Figures 3d–3g). For example, in the

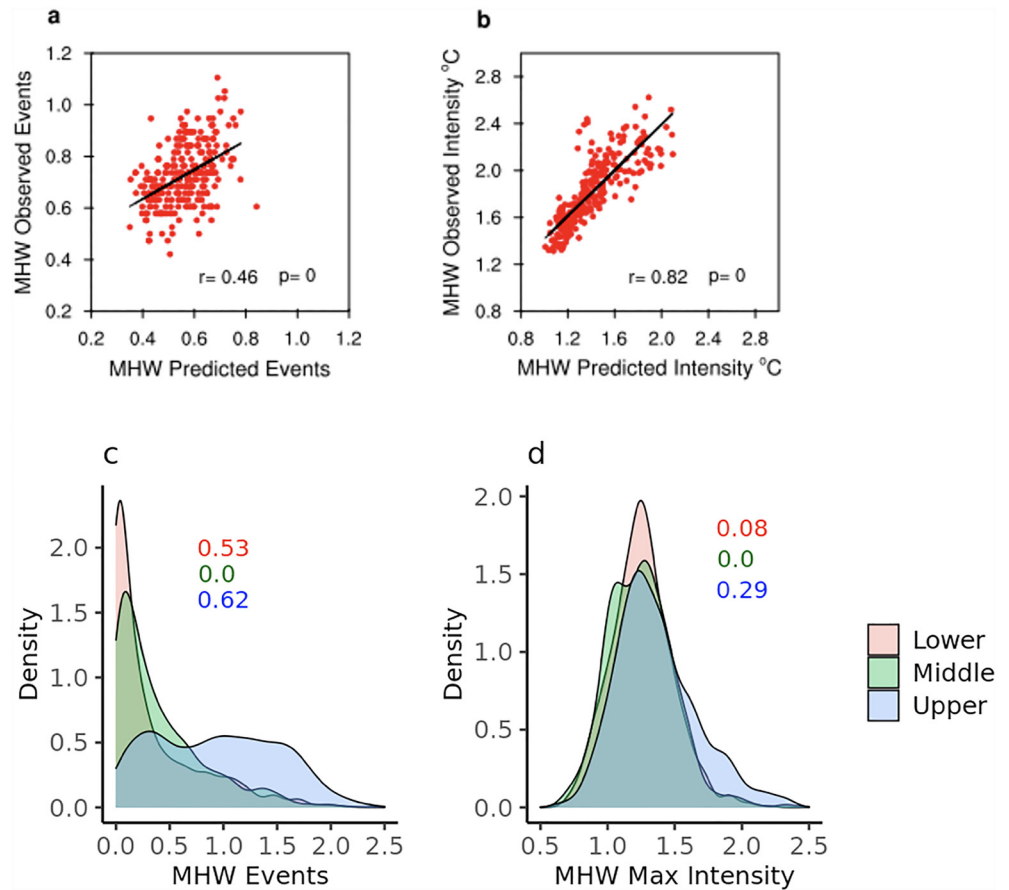


Figure 2. Seasonal prediction of marine heatwave characteristics. (a) Scatter plot for the predicted marine heatwave events per summer (June to August) against observations. Each dot represents the pair of values at the corresponding observation and model grid cell within the selected Arabian Sea region. (b) Same as (a) but for intensity. (c) Probability density functions of predicted marine heatwave events based on composite of observed percentiles of marine heatwave events. The numbers indicate the fraction of MHW predictions that were also in the same tercile as observations (see Table S3 in Supporting Information S1 for further details). (d) Same as (c) but for marine heatwave intensity.

summers of 1997, 2006, 2014 and 2017, MHW events occurred over more than half of the Arabian Sea region, making these summers as important as other summers with similar spatial coverage of MHW events and with El Niño as a precursor (Figures S4 and S5 in Supporting Information S1). To quantify the spatial coverage of MHW events, we calculate the area of Arabian Sea under heatwave each summer (Figure 4). Furthermore, we chose upper tercile as a threshold to identify summers when a “large” area of Arabian Sea experienced heatwave. With this definition, we identify a total of 13 summers when at least one MHW event occurred over a large area of Arabian Sea (red bars in Figure 4a).

To make this definition of MHW events more relevant to fisheries management, we combine the spatial information of MHW events with their intensity (Figure 4b). Here we use the occurrence of MHW and a fixed temperature threshold of 28°C relevant for the Indian oil sardine fishery, to compute the area under heatwave. Summers when absolute maximum intensity of heatwaves exceed 28°C for an extended period of time over a large area of Arabian Sea can be detrimental for Indian oil sardine fishery (Sajna et al., 2019). We see that when a large region of the Arabian Sea experiences heatwaves in summer, similarly large region also experiences temperatures larger than 28°C (Figure 4b, Figures S6 and S7 in Supporting Information S1). On average about 80% of the Arabian Sea region that experiences summer heatwaves also experiences temperatures larger than 28°C.

The 80-member hindcast is able to skilfully predict summers when a large area of Arabian Sea experiences heatwaves (Figure 4). These hindcasts are initialized in November and the prediction is verified in the summer from June to August, thus they provide a prediction horizon of seven months (see Methods). Similar skilful prediction

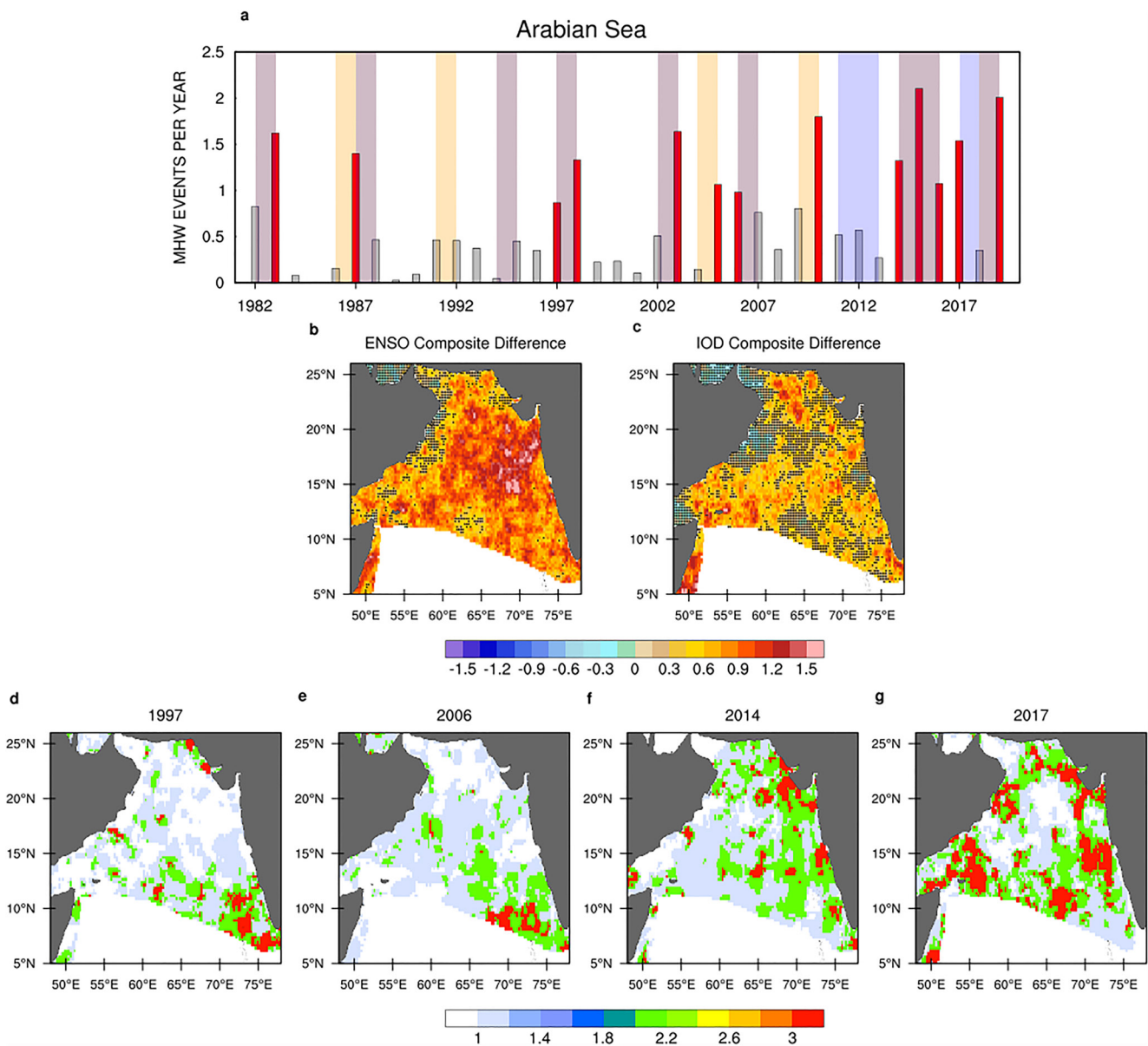


Figure 3. Impact of El Niño and IOD on occurrence of MHWs. (a) Time series of summer (June-August) mean MHW events averaged over the Arabian Sea. The orange shadings indicate El Niño periods and blue shadings indicate IOD+ periods (see Methods). The red bars denote summers when the MHW events were in the upper tercile. (b) Composite difference of MHW events between El Niño and non-El Niño years. (c) Same as (b) but for IOD+ and non-IOD+ years. Composite differences that are not significant at 95% confidence are stippled. (d–g) The four years (1997, 2006, 2014 and 2017) when the summer MHW events were in the upper tercile (red bars in (a)) without a preceding El Niño event.

is found for the area under heatwave using the combined event and intensity based definition. Irrespective of the definition, the skill is higher for predictions initialized in winters during an El Niño event than in other winters. This suggests that the prediction model is able to capture the impact of El Niño on the Arabian Sea seven months ahead.

Since there seems to be a connection between El Niño and MHWs over the Arabian Sea, we also compute the prediction skill from a statistical model based on winter SSTs in the Niño 3.4 region (see Methods). We use winter (Oct-Dec mean) Niño 3.4 SST anomaly as a predictor. The statistical model is skillful but its median skill is lower than that of the dynamical model. However, the statistical model also suggests the dependence of skill on El Niño—the skill is higher for summers preceded by an El Niño event in winter. Similar results are obtained if the statistical model is based on the IOD+ conditions (Figure S8 in Supporting Information S1). A detailed

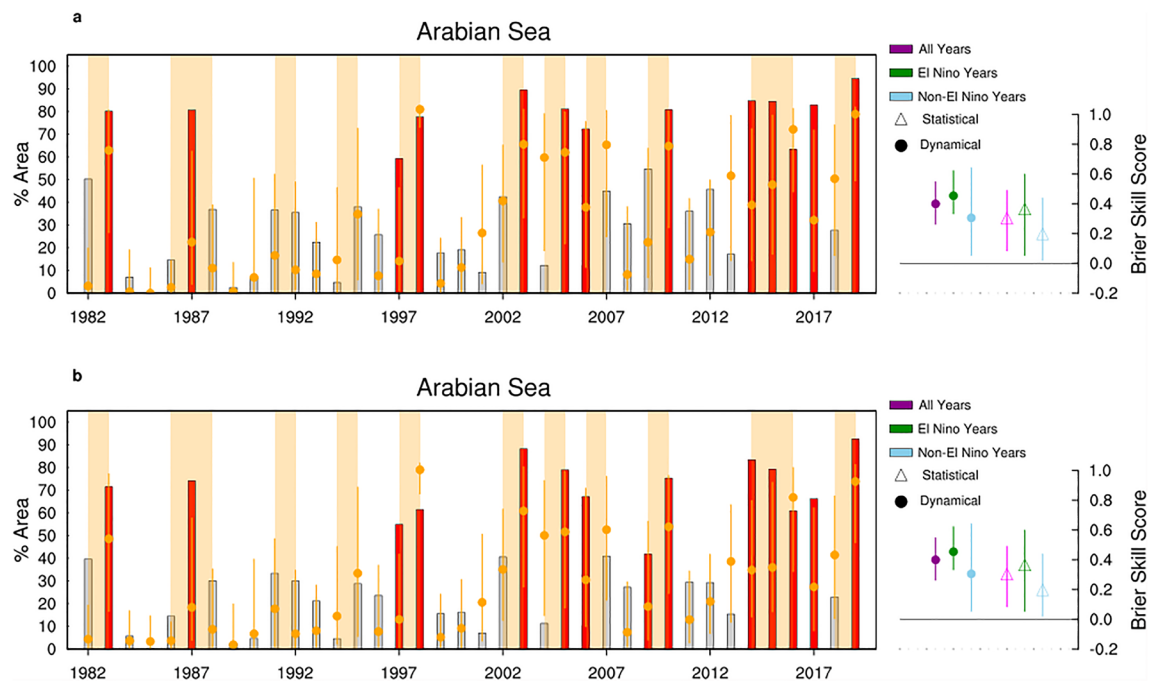


Figure 4. Seasonal prediction of area under marine heatwave. (a) Area under MHW from observation (bars) and the hindcasts (dots and whiskers) based on the events based definition (see Methods). The dots show the median prediction and the whiskers show the 90 percentile range from the 80-member ensemble. The orange shadings indicate El Niño periods. The right hand side panel shows the Brier skill score (BSS) for the dynamical and the statistical predictions computed from all years, El Niño years and non-El Niño years. Both BSSs are computed with the climatological prediction as reference. The circles and triangles show the respective median skill and the whiskers show the 90 percentile range from the bootstrap procedure (see Methods). (b) Same as (a) but for intensity-based definition of MHW.

analysis of individual years reveals that the dynamical model not only performs at par with the statistical model in summers preceded by an El Niño but also performs better in the absence of an El Niño in the preceding winter (Figures S9 and S10 in Supporting Information S1).

4. Discussion and Conclusions

Our main finding is that characteristics of summer MHWs in the Arabian Sea can be predicted seven months ahead. We find prediction skill for summers when a large area of the Arabian Sea experiences heatwaves, outperforming climatological predictions as well as an El Niño-based statistical model. The dynamical prediction model benefits from initialization in winters during an active El Niño, which facilitates an observationally consistent evolution of the climate. These findings are consistent with a recent report on the impact of ENSO on global prediction of MHWs (Jacox et al., 2022).

It is worth mentioning that the MHW calculation implemented here includes a 31-day smoothing of the 90th percentiles. This is done to smooth out any sub-seasonal variations in the daily temperature thresholds which might degrade the skill at seasonal timescales. Nevertheless, when the 31-day running mean is not employed, the skill remains largely unchanged. However, it remains to be seen whether there is any skill in predicting summer MHWs in the Arabian Sea at sub-seasonal timescales (2–4 weeks lead time).

In the Arabian Sea, summers with extensive MHWs are usually (but not always) associated with a preceding El Niño (or an IOD+ event) in winter. The mechanisms on how ENSO impacts SSTs in the Indian Ocean are largely understood (Chowdary & Gnanaseelan, 2007; Klein et al., 1999; Tourre & White, 1995). The remote teleconnection is realised via the changes in the Walker circulation which subsides over the western Indian Ocean during the El Niño. The subsidence reduces cloud cover and leads to an increase in incoming solar insolation which warms the sea surface. It is also important to note that subsidence over the Arabian Sea favors downwelling and inhibits ocean upwelling which can give rise to anomalous warming at the ocean surface (Pratik et al., 2019). Our finding that the likelihood of MHW occurrence increases in summers following an El Niño event in winter point to favorable background climate state set by such ENSO teleconnection. The higher skill in

summers following an El Niño event in winter indicates that the model is able to capture the impact of the decay phase of El Niño on the SST in the Arabian Sea. Caution should however be exercised when extrapolating the level of prediction skill presented here to the future. For example, the 1994 El Niño Modoki associated summer does not seem to show any MHW impact in the Arabian Sea. It remains to be seen how the projected changes in the ratio of El Niño Modoki to canonical El Niño events would impact MHWs and their prediction skill in the Arabian Sea (Marathe & Karumuri, 2021; Ying et al., 2022).

Previous studies suggest that MHWs can worsen negative impacts of the ongoing climate change on marine ecosystems and weaken the adaptive capacities of the latter to the decadal-scale temperature increase (Frölicher & Laufkötter, 2018; Weber et al., 2021; Wernberg et al., 2013). As specifically for the Arabian Sea, Cheung et al. (2021) estimated that between 25% and 50% of the commercially exploited fish stocks in this region will decline in biomass due a combined effect of long-term warming and increasing MHWs frequency in the future. This is expected to negatively affect the entire socio-economic system linked to the marine food industry. The MHW predictions presented here provide a critical time horizon necessary for precautionary measures that can mitigate the impact of such extreme events on marine ecosystems and promote a sustainable exploitation of marine resources. Such management measures can include, for example, a planned shift of fishery to the viable areas (seasons) not affected by MHWs, switching to alternative fish species and reducing fisheries activities to decrease the anthropogenic pressure on the spawning stock under unfavorable environmental conditions (Hobday, Spillman, et al., 2016; Payne et al., 2017).

However, a robust decision support tool for sardine fishery will require a further step to translate the physical forecast presented here to an ecological forecast predicting sardine distribution and recruitment success under various MHWs events. We see the lack of the precise information about the physiological response of oil sardines to suboptimally warm temperatures (Hamza, Anju, et al., 2021) as one of the main challenges in making such forecasts. The temperature threshold of 28°C used here was based on few previous studies, reporting disappearance of oil sardine from commercial catches at higher temperatures (Benzam, 1970; Vivekanandan et al., 2009). A better understanding of how suboptimal temperatures affect vital rates (growth, survival and reproduction) of the adult and pre-recruit oil sardine will be required. Given the observed and predicted increase of water temperature and MHWs intensity in summer in this region, we encourage further research combining fisheries independent surveys and laboratory experiments to elaborate on physiological and behavioral responses of oil sardines, as well as other key fish species and marine organisms prone to the devastating effects of MHWs.

Conflict of Interest

The authors declare no conflicts of interest relevant to this study.

Data Availability Statement

The NOAA 1/4° Daily Optimum Interpolation Sea Surface Temperature (OISST) data set is publicly available (<http://dx.doi.org/10.7289/V5SQ8XB5>). Model simulations are publicly available at World Data Center for Climate at DKRZ: <http://hdl.handle.net/hdl:21.14106/f2fdc61b13828ed5284f4e4ab41e63f8a84c6e52> (Brune et al., 2021), and <http://hdl.handle.net/hdl:21.14106/27e73ed39cd59d2033e018a494e342383db53a0b> (Brune et al., 2022).

References

- Andrew, B., Roy, C., & Lluch-Cota, S. (1998). Coastal upwelling and other processes regulating ecosystem productivity and fish production in the western Indian Ocean. *Large marine ecosystems of the Indian Ocean: assessment, sustainability, and management*, 17, 103–142.
- Babcock, R. C., Bustamante, R. H., Fulton, E. A., Fulton, D. J., Haywood, M. D., Hobday, A. J., et al. (2019). Severe continental-scale impacts of climate change are happening now: Extreme climate events impact marine habitat forming communities along 45% of Australia's coast. *Frontiers in Marine Science*, 411. <https://doi.org/10.3389/fmars.2019.00411>
- Banzon, V., Smith, T. M., Chin, T. M., Liu, C., & Hankins, W. (2016). A long-term record of blended satellite and in situ sea-surface temperature for climate monitoring, modeling and environmental studies. *Earth System Science Data*, 8(1), 165–176. <https://doi.org/10.5194/essd-8-165-2016>
- Benzam, P. (1970). On the fluctuations of the oil sardine fishery at kannanore during 1961–1964. *Indian Journal of Fisheries*, 17, 132–148.
- Bond, N. A., Cronin, M. F., Freeland, H., & Mantua, N. (2015). Causes and impacts of the 2014 warm anomaly in the ne pacific. *Geophysical Research Letters*, 42(9), 3414–3420. <https://doi.org/10.1002/2015gl063306>
- Brune, S., & Baehr, J. (2020). Preserving the coupled atmosphere–ocean feedback in initializations of decadal climate predictions. *Wiley Interdisciplinary Reviews: Climate Change*, 11(3), e637. <https://doi.org/10.1002/wcc.637>

Acknowledgments

This study is a contribution to the Excellence Cluster CliCCS - Climate, Climatic Change, and Society at the University of Hamburg, funded by the DFG through Germany's Excellence Strategy EXC 2037 Project 390683824 (JB and CS). This study is also a contribution to the PoF IV Program Changing Earth Sustaining our Future, Topic 4 Coastal Transition Zones under Natural and Human Pressure of the Helmholtz Association. JB and SB were supported by Copernicus Climate Change Service, funded by the EU, under contract C3S2-370. AD is supported by A4 (Aigéin, Aeráid, agus athrú Atlantaiagh), funded by the Marine Institute (Grant PBA/CC/18/01). AP is thankful to Niharika Shah, Veer Narmad South Gujarat University for scientific discussion. The authors thank the German Computing Center (DKRZ) for providing their computing resources. We acknowledge financial support from the Open Access Publication Fund of Universität Hamburg. Open Access funding enabled and organized by Projekt DEAL.

- Brune, S., Nerger, L., & Baehr, J. (2015). Assimilation of oceanic observations in a global coupled earth system model with the seik filter. *Ocean Modelling*, 96, 254–264. <https://doi.org/10.1016/j.ocemod.2015.09.011>
- Brune, S., Pohlmann, H., Müller, W. A., Nielsen, D. M., Hövel, L., & Baehr, J. (2021). MPI-ESM-LR_1.2.01p5 decadal predictions localEnKF: Daily mean values. Retrieved from <http://hdl.handle.net/hdl:21.14106/f2fdc61b13828ed5284f4e4ab41e63f8a84c6e52>
- Brune, S., Pohlmann, H., Müller, W. A., Nielsen, D. M., Hövel, L., Koul, V., & Baehr, J. (2022). MPI-ESM-LR_1.2.01p5 decadal predictions localEnKF large ensemble: Daily mean values members 17 to 80. Retrieved from <http://hdl.handle.net/hdl:21.14106/27e73ed39cd59d2033e018a494e342383db53a0b>
- Caputi, N., Kangas, M., Denham, A., Feng, M., Pearce, A., Hetzel, Y., & Chandrapavan, A. (2016). Management adaptation of invertebrate fisheries to an extreme marine heat wave event at a global warming hot spot. *Ecology and Evolution*, 6(11), 3583–3593. <https://doi.org/10.1002/ece3.2137>
- Cavole, L. M., Demko, A. M., Diner, R. E., Giddings, A., Koester, I., Pagnello, C. M., et al. (2016). Biological impacts of the 2013–2015 warm-water anomaly in the Northeast Pacific: Winners, losers, and the future. *Oceanography*, 29(2), 273–285. <https://doi.org/10.5670/oceanog.2016.32>
- Chatterjee, A., Anil, G., & Shenoy, L. R. (2022). Marine heatwaves in the Arabian Sea. *Ocean Science*, 18(3), 639–657. <https://doi.org/10.5194/os-18-639-2022>
- Cheung, W. W., Frölicher, T. L., Lam, V. W., Oyinola, M. A., Reygondeau, G., Sumaila, U. R., et al. (2021). Marine high temperature extremes amplify the impacts of climate change on fish and fisheries. *Science Advances*, 7(40), eabh0895. <https://doi.org/10.1126/sciadv.abh0895>
- Chowdary, J., & Gnanaseelan, C. (2007). Basin-Wide warming of the Indian Ocean during El Niño and Indian Ocean Dipole years. *International Journal of Climatology: A Journal of the Royal Meteorological Society*, 27(11), 1421–1438. <https://doi.org/10.1002/joc.1482>
- Feng, M., McPhaden, M. J., Xie, S.-P., & Hafner, J. (2013). La Niña forces unprecedented Leeuwin current warming in 2011. *Scientific Reports*, 3(1), 1–9. <https://doi.org/10.1038/srep01277>
- Filbee-Dexter, K., & Wernberg, T. (2018). Rise of turfs: A new battleground for globally declining kelp forests. *BioScience*, 68(2), 64–76. <https://doi.org/10.1093/biosci/bix147>
- Fröhlich, K., Dobrynin, M., Isensee, K., Gessner, C., Paxian, A., Pohlmann, H., et al. (2021). The German climate forecast system: GCFS. *Journal of Advances in Modeling Earth Systems*, 13(2), e2020MS002101. <https://doi.org/10.1029/2020MS002101>
- Frölicher, T. L., Fischer, E. M., & Gruber, N. (2018). Marine heatwaves under global warming. *Nature*, 560(7718), 360–364. <https://doi.org/10.1038/s41586-018-0383-9>
- Frölicher, T. L., & Laufkötter, C. (2018). Emerging risks from marine heat waves. *Nature Communications*, 9(1), 1–4. <https://doi.org/10.1038/s41467-018-03163-6>
- Hamza, F., Anju, M., Valsala, V., & Smitha, B. R. (2021a). A bioenergetics model for seasonal growth of Indian oil sardine (*sardinella longiceps*) in the Indian west coast. *Ecological Modelling*, 456, 109661. <https://doi.org/10.1016/j.ecolmodel.2021.109661>
- Hamza, F., Valsala, V., Malliserry, A., & George, G. (2021b). Climate impacts on the landings of Indian oil sardine over the south-eastern Arabian Sea. *Fish and Fisheries*, 22(1), 175–193. <https://doi.org/10.1111/faf.12513>
- Hobday, A. J., Alexander, L. V., Perkins, S. E., Smale, D. A., Straub, S. C., Oliver, E. C., et al. (2016a). A hierarchical approach to defining marine heatwaves. *Progress in Oceanography*, 141, 227–238. <https://doi.org/10.1016/j.poccean.2015.12.014>
- Hobday, A. J., Spillman, C. M., Paige Eveson, J., & Hartog, J. R. (2016b). Seasonal forecasting for decision support in marine fisheries and aquaculture. *Fisheries Oceanography*, 25, 45–56. <https://doi.org/10.1111/fog.12083>
- Hövel, L., Brune, S., & Baehr, J. (2022). Decadal prediction of Marine Heatwaves in MPI-ESM. *Geophysical Research Letters*, 49(15), e2022GL099347. <https://doi.org/10.1029/2022gl099347>
- Hughes, T. P., Kerry, J. T., Álvarez-Noriega, M., Álvarez-Romero, J. G., Anderson, K. D., Baird, A. H., et al. (2017). Global warming and recurrent mass bleaching of corals. *Nature*, 543(7645), 373–377. <https://doi.org/10.1038/nature21707>
- Jacox, M. G., Alexander, M. A., Amaya, D., Becker, E., Bograd, S. J., Brodie, S., et al. (2022). Global seasonal forecasts of marine heatwaves. *Nature*, 604(7906), 486–490. <https://doi.org/10.1038/s41586-022-04573-9>
- Klein, S. A., Soden, B. J., & Lau, N.-C. (1999). Remote sea surface temperature variations during ENSO: Evidence for a tropical atmospheric bridge. *Journal of Climate*, 12(4), 917–932. [https://doi.org/10.1175/1520-0442\(1999\)012<0917:rsstvd>2.0.co;2](https://doi.org/10.1175/1520-0442(1999)012<0917:rsstvd>2.0.co;2)
- Koul, V., Sguotti, C., Årthun, M., Brune, S., Düsterhus, A., Bogstad, B., et al. (2021). Skilful prediction of cod stocks in the north and Barents Sea a decade in advance. *Communications Earth & Environment*, 2(1), 1–10.
- Kripa, V., Mohamed, K. S., Koya, K. S., Jeyabakaran, R., Prema, D., Padua, S., et al. (2018). Overfishing and climate drives changes in biology and recruitment of the Indian oil sardine *sardinella longiceps* in southeastern Arabian Sea. *Frontiers in Marine Science*, 5, 443. <https://doi.org/10.3389/fmars.2018.00443>
- Marathe, S., & Karumuri, A. (2021). The El Niño Modoki. In *Tropical and extratropical air-sea interactions* (pp. 93–114). Elsevier.
- Mauritsen, T., Bader, J., Becker, T., Behrens, J., Bittner, M., Brokopf, R., et al. (2019). Developments in the MPI-M Earth system model version 1.2 (MPI-ESM1.2) and its response to increasing CO₂. *Journal of Advances in Modeling Earth Systems*, 11(4), 998–1038. <https://doi.org/10.1029/2018MS001400>
- Nerger, L., & Hiller, W. (2013). Software for ensemble-based data assimilation systems—Implementation strategies and scalability. *Computers & Geosciences*, 55, 110–118. <https://doi.org/10.1016/j.cageo.2012.03.026>
- Olita, A., Sorgente, R., Natale, S., Gaberšek, S., Ribotti, A., Bonanno, A., & Patti, B. (2007). Effects of the 2003 European heatwave on the central Mediterranean Sea: Surface fluxes and the dynamical response. *Ocean Science*, 3(2), 273–289. <https://doi.org/10.5194/os-3-273-2007>
- Oliver, E. C. (2019). Mean warming not variability drives marine heatwave trends. *Climate Dynamics*, 53(3), 1653–1659. <https://doi.org/10.1007/s00382-019-04707-2>
- Oliver, E. C., Benthuyens, J. A., Bindoff, N. L., Hobday, A. J., Holbrook, N. J., Mundy, C. N., & Perkins-Kirkpatrick, S. E. (2017). The unprecedented 2015/16 Tasman Sea marine heatwave. *Nature Communications*, 8(1), 1–12. <https://doi.org/10.1038/ncomms16101>
- Oliver, E. C., Burrows, M. T., Donat, M. G., Sen Gupta, A., Alexander, L. V., Perkins-Kirkpatrick, S. E., et al. (2019). Projected marine heatwaves in the 21st century and the potential for ecological impact. *Frontiers in Marine Science*, 6, 734. <https://doi.org/10.3389/fmars.2019.00734>
- Payne, M. R., Hobday, A. J., MacKenzie, B. R., Tommasi, D., Dempsey, D. P., Fässler, S. M. M., et al. (2017). Lessons from the first generation of marine ecological forecast products. *Frontiers in Marine Science*, 4, 289. <https://doi.org/10.3389/fmars.2017.00289>
- Pearce, A. F., & Feng, M. (2013). The rise and fall of the “marine heat wave” off Western Australia during the summer of 2010/2011. *Journal of Marine Systems*, 111, 139–156. <https://doi.org/10.1016/j.jmarsys.2012.10.009>
- Pratik, K., Parekh, A., Karmakar, A., Chowdary, J. S., & Gnanaseelan, C. (2019). Recent changes in the summer monsoon circulation and their impact on dynamics and thermodynamics of the Arabian Sea. *Theoretical and Applied Climatology*, 136(1), 321–331. <https://doi.org/10.1007/s00704-018-2493-6>

- Sajna, V. H., Zacharia, P. U., Liya, V. B., Rojith, G., Somy, K., Joseph, D., & Grinson, G. (2019). Effect of climatic variability on the fishery of Indian oil sardine along Kerala coast. *Journal of Coastal Research*, 86(SI), 184–192. <https://doi.org/10.2112/si86-028.1>
- Saranya, J., Roxy, M. K., Dasgupta, P., & Anand, A. (2022). Genesis and trends in marine heatwaves over the tropical Indian Ocean and their interaction with the Indian summer monsoon. *Journal of Geophysical Research: Oceans*, 127(2), e2021JC017427. <https://doi.org/10.1029/2021jc017427>
- Sherman, K. (1991). The large marine ecosystem concept: Research and management strategy for living marine resources. *Ecological Applications*, 1(4), 349–360. <https://doi.org/10.2307/1941896>
- Smale, D. A., Wernberg, T., Oliver, E. C., Thomsen, M., Harvey, B. P., Straub, S. C., et al. (2019). Marine heatwaves threaten global biodiversity and the provision of ecosystem services. *Nature Climate Change*, 9(4), 306–312. <https://doi.org/10.1038/s41558-019-0412-1>
- Tourre, Y. M., & White, W. B. (1995). Enso signals in global upper-ocean temperature. *Journal of Physical Oceanography*, 25(6), 1317–1332. [https://doi.org/10.1175/1520-0485\(1995\)025<1317:esiguo>2.0.co;2](https://doi.org/10.1175/1520-0485(1995)025<1317:esiguo>2.0.co;2)
- Vivekanandan, E., Rajagopalan, M., & Pillai, N. G. K. (2009). Recent trends in sea surface temperature and its impact on oil sardine. *Global Climate Change and Indian Agriculture*, 17, 89–92.
- Weber, E. D., Auth, T. D., Baumann-Pickering, S., Baumgartner, T. R., Bjorkstedt, E. P., Bograd, S., et al. (2021). State of the California current 2019–2020: Back to the future with marine heatwaves? *Frontiers in Marine Science*, 8, 709454. <https://doi.org/10.3389/fmars.2021.709454>
- Wernberg, T., Russell, B. D., Thomsen, M. S., Gurgel, C. F. D., Bradshaw, C. J., Poloczanska, E. S., & Connell, S. D. (2011). Seaweed communities in retreat from ocean warming. *Current Biology*, 21(21), 1828–1832. <https://doi.org/10.1016/j.cub.2011.09.028>
- Wernberg, T., Smale, D. A., Tuya, F., Thomsen, M. S., Langlois, T. J., de Bettignies, T., et al. (2013). An extreme climatic event alters marine ecosystem structure in a global biodiversity hotspot. *Nature Climate Change*, 3(1), 78–82. <https://doi.org/10.1038/nclimate1627>
- Ying, J., Collins, M., Cai, W., Timmermann, A., Huang, P., Chen, D., & Stein, K. (2022). Emergence of climate change in the tropical Pacific. *Nature Climate Change*, 12(4), 356–364. <https://doi.org/10.1038/s41558-022-01301-z>